ISBN: 978-3-95450-232-5 ISSN: 2673-7000 doi:10.18429/JACoW-NAPAC2022-WEPA72

ANALYSIS OF BEAM-INDUCED HEATING OF THE NSLS-II CERAMIC VACUUM CHAMBERS

G. Bassi*, A. Khan, B. Kosciuk, V. Smaluk, R. Todd, C. Hetzel, M. Seegitz, A. Blednykh
Brookhaven National Laboratory, Upton, NY, USA

Abstract

We discuss the impedance and related beam-induced heating issues of the titanium coated ceramic vacuum chambers of the NSLS-II storage ring. The impedance of the two-layer electromagnetic system is calculated assuming a parallel plate model using the well known Field Matching Theory (FMT) and compared with the IW2D code. It is demonstrated that for the chamber coating thickness of interest, all power is dissipated on the titanium coating, with the longitudinal averaged two-dimensional power density independent on the vertical direction and Gaussian-distributed along the horizontal direction with a standard deviation equal to the thickness of the ceramic layer. These properties allow for a simplified model of the power density as input of ANSYS simulations for thermal analysis and comparison with measurements.

INTRODUCTION

To estimate the effects of shielding and impedances on power loss, it is important to find a reasonable thickness of Ti coating on a ceramic chamber [1]. Several accelerators including BESSY-II [2], ESRF [3], HLS [4], MAX-IV [5] and NSLS-II [6] stated overheating of their Ti coated ceramic chambers, which has been reported due to lack of coating uniformity with appropriate thickness or/and poor coating adhesion. Therefore, to avoid failure of ceramic chambers due to thermal stress cracking for a given ceramic shape and loss tangent, a sequence of simulations are usually performed to calculate the EM fields, impedance, heat source distribution, temperature map, and stress field.

At NSLS-II, one of the crucial milestone to achieve the 500 mA design current was the ceramic chambers, because of their overheating. The effect was mitigated by installing additional cooling fans [6, 7].

In this work, we discuss the field matching theory to compute the impedance of multi-layered chambers and compared it with the IW2D code. Further, we discuss the power density distribution for such chambers which is used for thermal analysis in ANSYS.

FIELD MATCHING THEORY

We assume the model shown in Fig. 1. Following the analytical approach adopted in [8], we extended the theory to consider the most general electromagnetic properties of the two-layer (metal-ceramics) system [9]. Assuming the two layers characterized by the complex relative permittivity $\hat{\varepsilon}_{1r}$, $\hat{\varepsilon}_{2r}$, and complex relative permeability $\hat{\mu}_{r1}$, $\hat{\mu}_{r2}$, where

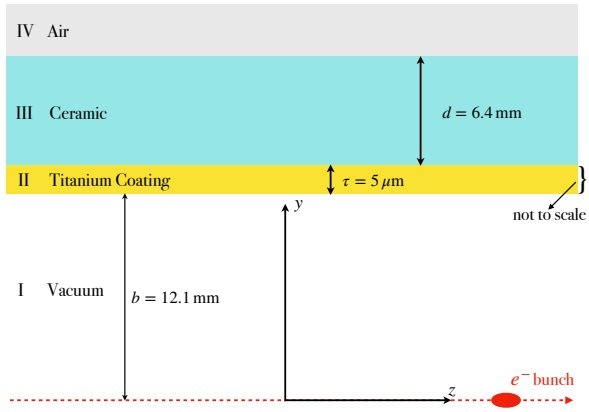

Figure 1: Geometry of the vacuum chamber in planar approximation. All the parameters correspond to the NSLS-II ceramic chamber with the Ti coating thickness value shown for illustration purpose.

the index 1 and 2 refers to the metal and ceramic layer respectively, it can be shown that the longitudinal impedance per unit length can be calculated using the following formula

$$\frac{Z_0^{\parallel}(k)}{L} = -i\frac{Z_0}{4\pi}k\int_{\infty}^{+\infty}\frac{F(k,q)}{G(k,q)}dq, \qquad (1)$$

where F is independent on b and G can be written in the form

$$G(k,q) = w_0 + w_1\cosh 2bq + w_2\sinh 2bq, \qquad (2)$$

where w_0, w_1 and w_2 are also independent on b. The functions F, w_0, w_1 and w_2 are not shown here and are given in [9].

Table 1: Material properties of Ti coated ceramic chambers. The value of the Ti coating thickness is shown for just of the ceramic chambers.

Layers	ρ [Ωm]	$\tan(\delta)$	ϵ'	τ [mm]
Ti	4.3×10^{-7}	0	1	1.21×10^{-3}
Ce	0	1×10^{-3}	10	6.4
Air	2×10^{16}	0	1	Infinity

Benchmarking Field Matching Theory against IW2D simulations

We compare the FM theory with IW2D, a code developed at CERN to compute longitudinal and transverse impedance

* gbassi@bnl.gov

ISBN: 978-3-95450-232-5 ISSN: 2673-7000 doi:10.18429/JACoW-NAPAC2022-WEPA72

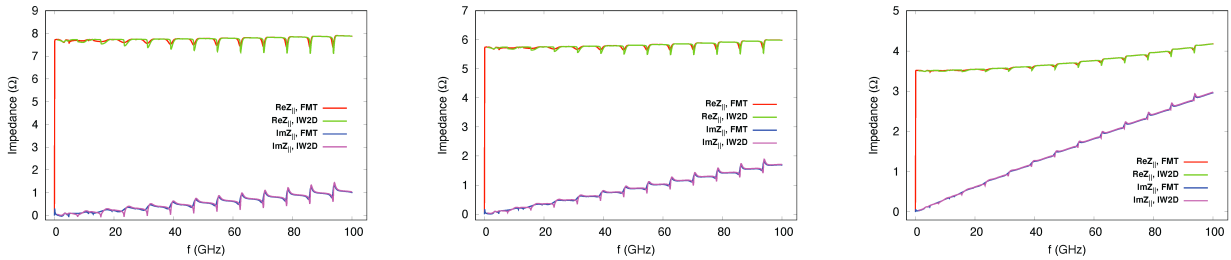

Figure 2: Comparison of the Ti coated ceramic chamber impedance for coating thickness of $\tau = 0.55$, 0.74, and 1.21 µm with IW2D and FMT.

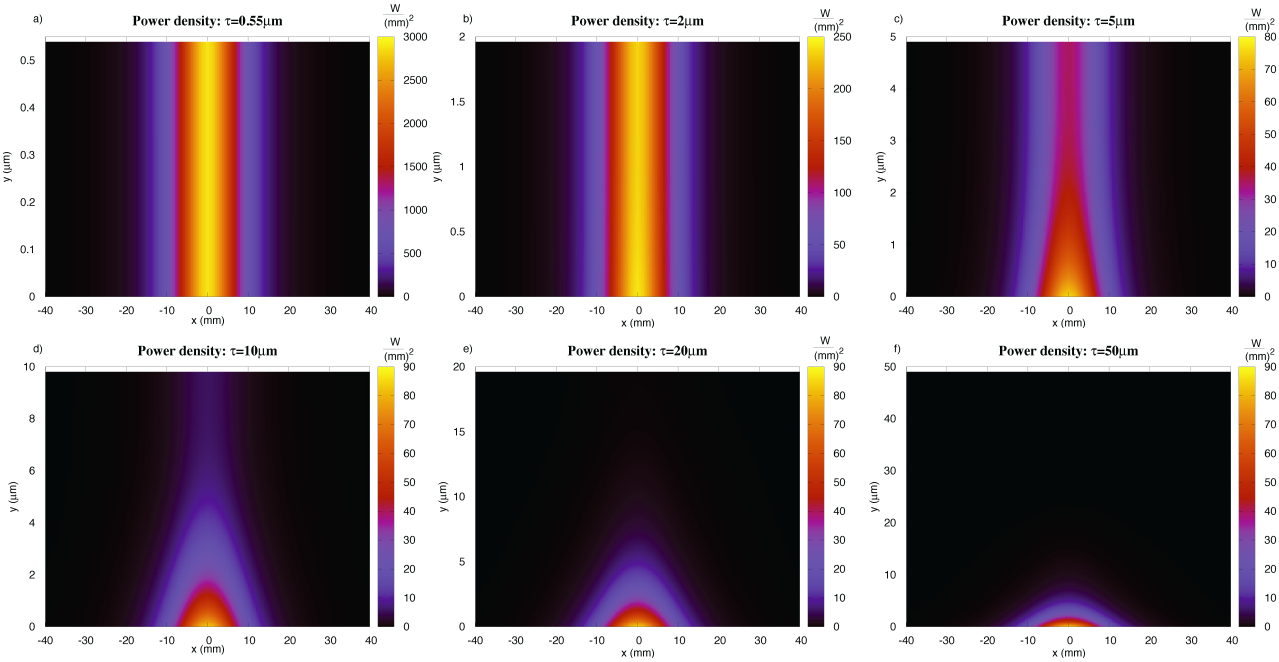

Figure 3: 2D-power density (longitudinal averaged) as a function of the transverse coordinates for several values of the Ti coating thickness. Below 2 µm, the power density is uniform in y with a Gaussian horizontal profile with $\sigma_x = d$, where d is the thickness of the ceramic chamber.

in a two-dimensional multi-layered flat structure. The number of layers can be arbitrary depending on the user application requirement, and each of them can be made of any linear homogeneous isotropic stationary material. The last layer (which can also be vacuum) should always be modeled with infinite thickness and with low conductivity. The code relies on the analytic computation of the electromagnetic fields created by a point-charge beam traveling at any speed in the whole structure. The details of the flat structure impedance formalism are discussed in [15, 16].

We simulate the NSLS-II chambers of radius $b = 12.1$ mm as a 3-layer flat structure composed of a 6.4 mm thickness ceramic chamber with three different values of Ti coating $\tau = 0.55, 0.74, 1.21$ µm, plus the last infinite layer. The material properties for the IW2D calculations are given in Table 1. Figure 2 shows the comparison of the longitudinal impedance obtained from IW2D and FMT of the NSLS-II chambers with different Ti coating thickness. A good agreement is found between the theory and IW2D calculations.

2D-POWER DENSITY AND THERMAL ANALYSIS

The FMT discussed in the previous Section allows for the determination of the electromagnetic fields anywhere, thus allows for the calculation of the average longitudinal two-dimensional power density as a function of the transverse coordinates (x, y). The derivation of the analytical formula is not discussed here at can be found in Ref. [9]. Figure 3 shows the average longitudinal two-dimensional power density on the metal coating as a function of the coating thickness. Below ~2 µm, the two-dimensional power density is independent on the vertical direction and has an horizontal Gaussian profile with $\sigma_x = d$, where d is the thickness of the ceramic chamber. Figure 4 (left frame) shows the total power dissipated on the titanium coating as a function of the coating thickness. For the coating thickness in the range shown in the figure, all the power is dissipated on the metal coating and is roughly equal to the total power lost by the beam. Figure 4 (center frame) shows the thermal

ISBN: 978-3-95450-232-5 ISSN: 2673-7000 doi:10.18429/JACoW-NAPAC2022-WEPA72

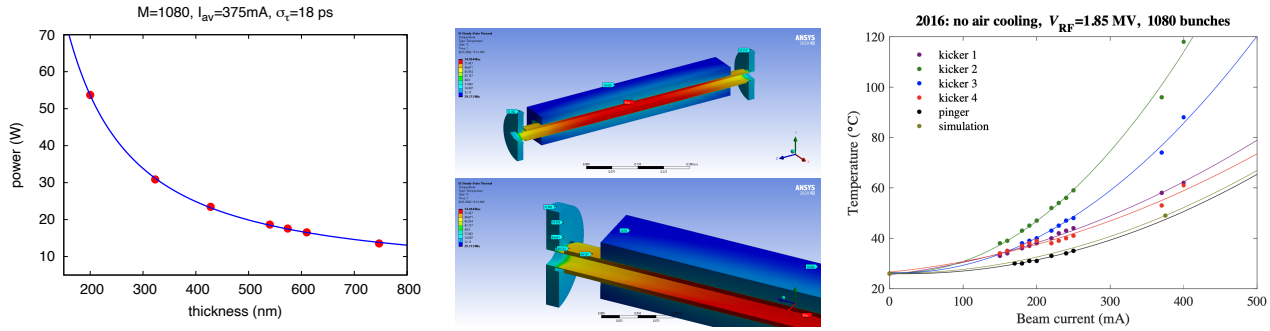

Figure 4: Total power dissipated on the titanium coating vs. coating thickness (left). Thermal simulations with ANSYS for the kicker 2 chamber with coating thickness of 428 nm (center). Temperature increase vs. beam current for the different ceramic chambers (right). The point in dark green color corresponds to the ANSYS simulated temperature, to be compared with the measured value of kicker 2 (light green color). The lines shown in the right frame correspond to a nonlinear fit of the measured values.

analysis for the kicker 2 chamber with coating thickness of 428 nm and Figure 4 (right frame) shows the temperature increase vs. beam current of the NSLS-II ceramic chambers measured during operations with $M = 1080$ bunches and $I_{av} = 375$ mA, and bunch length $\sigma_\tau = 18$ ps. The ANSYS simulated temperature of the kicker 2 ceramic chamber close to the location of the temperature sensors is 50° C, as shown in Figure 4 (right frame) by the dot in dark green color, to be compared with the measured value of 95° C shown by the dot in light green color.

CONCLUSION

We discussed an analytical model that allows for the calculation of the power density on the ceramic chamber metal coating. The power density is then used by ANSYS for thermal analysis, which allows for a comparison with measurements. We observed a discrepancy between the simulated and measured temperatures. The origin of such a discrepancy is under investigation and might be related to the uncertainty of the measured thickness and uniformity of the Ti coating. Also, the choice of the parameters used in the thermal simulations with ANSYS might explain the disagreement between measurements and simulations.

REFERENCES

[1] U. Iriso, T. F. G. Günzel, H. Bartosik, E. Koukovini-Platia, and G. Rumolo, "Beam-based Impedance Characterization of the ALBA Pinger Magnet," in *Proc. IPAC'15*, Richmond, VA, USA, May 2015, pp. 334–337. doi:10.18429/JACoW-IPAC2015-MOPJE027

[2] O. Dressler, T. Atkinson, M. Dirsat, P. Kuske, and H. Rast, "Development of a Non-Linear Kicker System to Facilitate a New Injection Scheme for the BESSY II Storage Ring," in *Proc. IPAC'11*, San Sebastian, Spain, Sep. 2011, pp. 3394–3396. https://jacow.org/IPAC2011/papers/THPO024.pdf

[3] S. White, *Collective effects at ESRF*, https://meetings.triumf.ca/event/254/contributions/3129/attachments/2414/2764/EIC_CollectiveEffects.pdf, [EIC Workshop'21], 2021.

[4] D. Xu and W. Xu, "Study on beam-induced heating in injection section of Hefei Light Source," *J. Phys.: Conf. Series*, vol. 1350, p. 012 018, 2019. doi:10.1088/1742-6596/1350/1/012018

[5] J. Kallestrup *et al.*, "Studying the Dynamic Influence on the Stored Beam From a Coating in a Multipole Injection Kicker," in *Proc. IPAC'19*, Melbourne, Australia, May 2019, pp. 1547–1550. doi:10.18429/JACoW-IPAC2019-TUPGW063

[6] A. Blednykh *et al.*, "Beam-Induced Heating of the Kicker Ceramics Chambers at NSLS-II," in *Proc. NAPAC'16*, Chicago, IL, USA, Oct. 2016, pp. 599–601. doi:10.18429/JACoW-NAPAC2016-TUPOB50

[7] C. Laasch, *NSLS-II Achieves Design Beam Current of 500 Milliamperes*, 2020. https://www.bnl.gov/nsls2/newsletter/news.php?a=217026

[8] A. Blednykh, G. Bassi, Y. Hidaka, V. Smaluk, and G. Stupakov, "Low-frequency quadrupole impedance of undulators and wigglers," *Phys. Rev. Accel. Beams*, vol. 19, p. 104 401, 2016. doi:10.1103/PhysRevAccelBeams.19.104401

[9] G. Bassi, "Impedance analysis and power dissipation of a metallic coated ceramic vacuum chamber," in preparation, 2022.